Emergent Scientist **3**, 3 (2019)
© J. André et al., Published by EDP Sciences, 2019
https://doi.org/10.1051/emsci/2019002

Emergent Scientist

Available online at:
www.emergent-scientist.edp-open.org

IPT 2018

RESEARCH ARTICLE OPEN ACCESS

Motion of rain drops on a car side window

Julie André[1,*], Clément Brochet[1], Quentin Louis[1], Amaury Barral[1], Anthony Guillen[1], Fang-Ting Goh[1], Angel Prieto[1], and Thibault Guillet[2]

[1] Ecole polytechnique, 91128 Palaiseau, France
[2] LadHyX, UMR 7636, CNRS, Ecole polytechnique, 91128 Palaiseau, France

Received: 24 June 2018 / Accepted: 11 February 2019

Abstract. The present paper studies the initial motion of rain drops on a car side window. An explanation to the common observation of drops going up the window when a car reaches a given speed is provided, which takes into account the dimensions of the drops and the wind speed. We also discuss the importance of the actual window geometry, the state of the surface, and the drop size distribution. This work may thus be used as a basis for complete study of a population of drops against a car window.

Keywords: Drop / trajectory / car / wind / adhesion

1 Introduction

You will have probably already noticed a puzzling phenomenon while driving your car in the rain: on the side-windows of a moving car, rain drops may adopt a wide range of behaviors and trajectories, as shown in Figure 1, some of them stay at rest, while others tend to move either downwards or upwards. The purpose of this study is to identify those different regimes of behaviors and to explain the observed trajectories.

The motion of rain drops on a car is of tremendous interest, since if they stick on the glass they limit the visibility through the window, which may trigger safety issues. This subject is therefore greatly interesting the automobile field. Another subject, important for visibility issues and quite close to the dynamic of drops on a car window, is the formation and stability of thin films and rivulets, such as the localized canals observed in Figure 1. This subject has already been closely studied [1–4] and will not be consider in this paper.

The dynamic of drops on a plane surface has been investigated usually in simpler conditions: the influence of gravity [5] and drag force [6,7] has been separately looked at. A thorough study of the parameters involved in the drag force can be found in [1]. The specific problem of a car window also involves aerodynamic effects such as side vortices, which have been meticulously studied in [8]. The subject concerning drops on a car side window has been studied in [9,10], where emphasis was put on removing drops from the glass to enhance visibility. However, none of those studies have tackled the determination of the drops' trajectories.

In this paper, we will focus on the trajectories of rain drops once they are on the side windows, where all the forces mentioned above must be taken into account. We first present our method to model the dynamics of a drop undergoing gravity, drag forces and capillarity forces (due to the interaction of the drop with the surface). Experimental results are then provided and enable us to validate the models and explain the different regimes observed on a car window. We finally discuss how our model could be used as a basis to study a whole population of drops on a car window, where the geometry of the car, surface treatment and drop merging play crucial roles.

2 Methods

Hypothesis: we consider a single drop holding on a car side window. We assume that the car is driven with a constant speed on a straight line (so that it can be considered as an inertial frame of reference) and that we have access to the local wind on the car window (value and direction).

We then intend to find:
– the conditions needed to dislodge the drop;
– the direction taken by the drop once dislodged;
– the conditions forcing its trajectory to have an upward component.

2.1 Forces acting on a drop

Different forces are acting on this drop: the weight $\vec{P}$, the adhesion force of the window $\vec{F}_{\mathrm{ad}}$, the drag force $\vec{F}_w$

* e-mail: julie.andre.2016@polytechnique.org

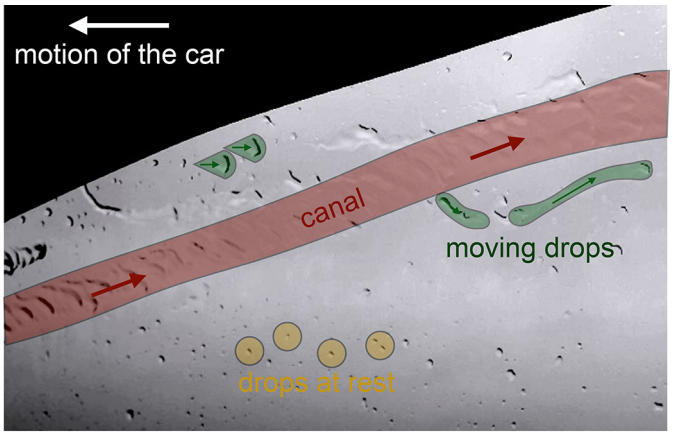

Fig. 1. Picture of rain drops on the side window of a moving car. The drops have different trajectories; some of them are going up, other have almost horizontal directions. Merging between drops occur, which makes the different paths quite erratic. The wetting of the window makes it easier to take some predefined paths (canals), as we can see on the top part on the window.

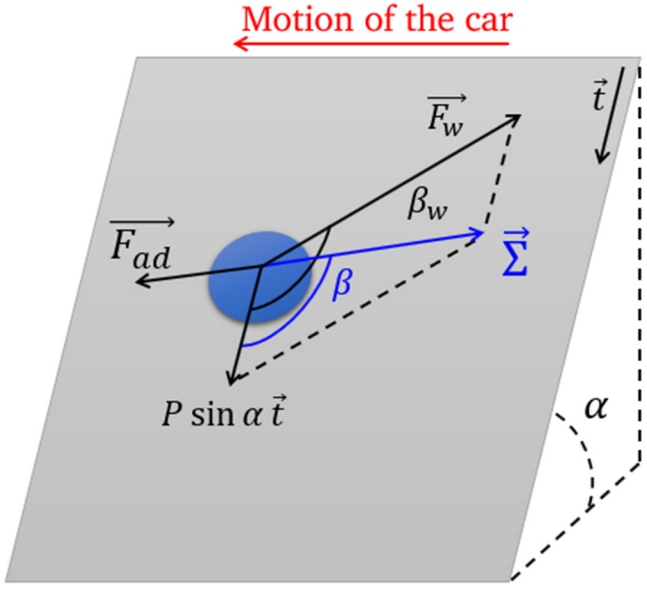

Fig. 2. Schematic view of the three forces applying on a drop, holding on a tilted plane of inclination α and under a wind of given direction β_w on the plane. $\vec{t}$ is an unit vector tangential to the plane. The sum $\vec{\Sigma}$ of the two external forces (weight $P\sin\alpha\,\vec{t}$ and drag force $\vec{F}_w$) is represented in blue. The angle between $\vec{\Sigma}$ and $\vec{t}$ is defined as β.

exerted by the wind, and the shear force within the drop. In our situation, the shear force within the drop when it deforms is negligible, since the drop deforms slowly and can therefore be considered as quasi-static. As long as the drop is at rest, there is a mechanical equilibrium in the plane of the window. Thus, one has: $(\vec{P}\cdot\vec{t})\vec{t} + \vec{F}_w + \vec{F}_{\rm ad} = \vec{0}$, where $\vec{t}$ denotes a unit vector tangential to the plane, directed downwards. Figure 2 sums up the situation.

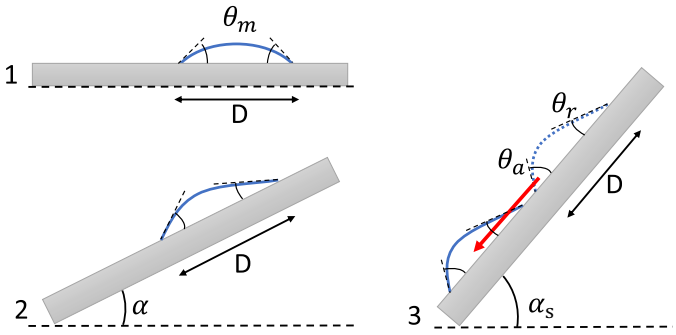

Fig. 3. Schematic representations of : (1) a drop of diameter D on a horizontal plane, (2) its deformation under gravity, when the plane which is progressively inclined and (3) the moment when the drop begins to slide. θ_a is the advancing angle and θ_r the receding angle.

2.2 Dislodging a drop

To dislodge the drop, the adhesion force must be overtaken by the two external forces. This gives the general condition of sliding:

$$||P\sin\alpha\,\vec{t} + \vec{F}_w|| \geq F_{\rm ad} \qquad (1)$$

where α denotes the inclination angle of the plane. We began by considering two simpler cases where only one external force out of the two plays a role: first, the weight, then the drag force, which can both lead to the dislodgement of the drop.

2.3 Influence of the weight: theoretical prediction

The following part models the competition between weight and adhesion forces, when the wind speed is null. The expression of weight is well known: $P = \Omega\rho_{\rm water}g$ with Ω the volume of the drop, $\rho_{\rm water}$ the density of water and g the gravity. To derive a model for the adhesion force, we need to explain why a drop can hold on an inclined plane.

While a still drop on a horizontal plane has a perfectly symmetric shape, it deforms and becomes asymmetric if one inclines the plane: the contact angle varies along the perimeter of the drop, see Figure 3. MacDougall and Ockrent [11] and then Furmidge [5] have elaborated a simple model to explain this: the drop can deform to minimize its energy when submitted to an external force (such as weight or wind drag) and to capillarity forces sticking it on the surface; the asymmetry of contact angles enables the drop to hold on the tilted plane. The drop's deformation is limited. When the contact angle at the front reaches the maximum angle θ_a then the contact line advances: θ_a is thus defined as the advancing angle. On the other hand, when the contact angle at the back reaches the minimum angle θ_r, the contact line retracts, therefore θ_r is defined as the receding angle. The drop will start sliding when θ_r and θ_a are both reached on two opposite sides of the drop, see Figure 3.

According to Furmidge, the maximum adhesion force can be modeled at the first order as $F_{\text{ad}} = \gamma(\cos\theta_r - \cos\theta_a)D$, where γ is the surface tension of water and D is the diameter of the drop. This maximum adhesion force is reached when the drop is the most asymmetric, and after that, it starts sliding.

Hence, just before sliding the mechanical equilibrium of the drop on a plane with maximum inclination α_s reads: $P\sin\alpha_s = F_{\text{ad}}$. This gives us a relation between this inclination and the drop's volume Ω:

$$\rho\Omega g\sin\alpha_s = \gamma(\cos\theta_r - \cos\theta_a)D \tag{2}$$

2.4 Influence of the weight: experimental setup

For the first set of experiments, we used an acrylic board (made of polymethyl methacrylate) as a support for the drops, which we cleaned with ethanol to make the experiment reproducible. With a μL-pipette, we injected a drop of known volume Ω (ranging from 15 μL to 100 μL) on the plane. By taking a picture of it from above, we had access to the drop diameter D (approximately between 4 mm and 10 mm). Then, we inclined the plane slowly (doing so, the projection of the weight on the plane increases) up to the angle α_s where the drop slides. The angle of sliding α_s may theoretically vary from 0° (superhydrophobic behavior) to 90° (the drop is stuck on the surface whatever the angle α).

2.5 Dislodging a drop with drag force: theoretical prediction

In the following part, we investigate the influence of the wind blowing on a horizontal plane, where a single drop of volume Ω is lying. Equilibrium is obtained similarly to the situation where the drop is undergoing gravity: adhesion forces equalize the drag force up to a maximum deformation of the drop. When the drag force increases beyond the maximum adhesion force, the drop begins to slide in the direction imposed by the wind. We now want to obtain a consistent estimate of the drag force.

We first consider a spot at a distance x from the edge of the plane, under a wind blowing horizontally. The Reynolds number $\text{Re}(x) = \frac{x.u}{\nu_a}$ with ν_a the kinematic viscosity of air, at $x \approx 10$ cm from the edge of the plane and with an air velocity $u = 10$ m/s is about 10^4. For such high Reynolds number, the boundary layer thickness $\delta(x)$ follows with good approximation the law established by Prandtl [12]: $\delta(x) = \sqrt{\nu_a x/u}$. This yields $\delta(x) \approx 0.5$ mm at a distance $x \approx 10$ cm from the edge of the plane. If a drop of diameter $D \approx 1$ cm sits on this spot, as we have $D/\delta \gg 1$, we can consider the local wind speed u on the drop to be uniform.

As the Reynolds number of the flow around the drop $\text{Re}(D) = \frac{D.u}{\nu_a} \approx 10^4$ is great compared to 1, the expression of the drag force is thus $F_w = \frac{1}{2}C_x\rho_a S u^2$ (as can be found in [13]), with C_x the horizontal drag coefficient, independent of Re, linked to the drop geometry, ρ_a the air volume weight and S the surface of the drop projected on the plane perpendicular to the direction of the wind.

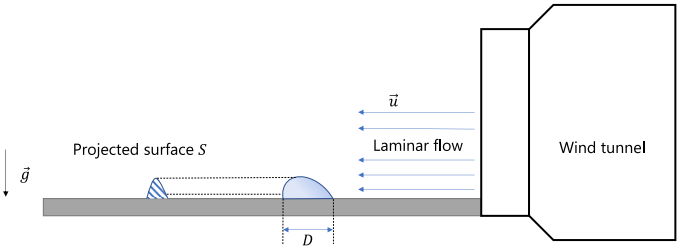

Fig. 4. Schematic view of the experiment to dislodge a horizontal drop with drag force. We use a wind tunnel, to ensure that the air flow is laminar and to shrink wind speed variability. The wind could blow from 1 to 30 m s^{-1}.

Finally, the equilibrium of the adhesion force and the drag force gives:

$$\frac{1}{2}C_x\rho_a S u_s^2 = \gamma(\cos\theta_r - \cos\theta_a)D. \tag{3}$$

From which we can deduce the speed of the wind u_s needed to force a given still drop to slide on a horizontal plane:

$$u_s^2 = \frac{2\gamma(\cos\theta_r - \cos\theta_a)D}{C_x\rho_a S}. \tag{4}$$

2.6 Dislodging a drop with drag force: experimental setup

For this second set of experiments, we used the same acrylic board as described above, kept horizontal. We injected drops of given volume Ω and measured diameter D (respectively between 5μL and 100 μL and from 3 mm to 11 mm) on the plane. We then switched on the wind blower and increased the wind speed until the drops began to slide. Wind speeds ranged from 5 m s^{-1} to a maximum value of 25 m s^{-1}. The wind blower had a precision of 0.5 m s^{-1}, see Figure 4.

2.7 Direction of the drop once dislodged: theoretical prediction

Now we assume that the drop has been dislodged under the combined action of gravity and wind, as shown in Figure 2. The adhesion force is a reaction force having the same direction that the sum of the external forces $\vec{\Sigma} = \vec{P} + \vec{F}_w$. The drop thus follows the direction of the resulting global force $\vec{\Sigma} + \vec{F}_{\text{ad}}$, which is in the direction of $\vec{\Sigma}$. To have access to the angle β taken by the drop, we can project $\vec{\Sigma}$ on the plane, which gives:

$$\cos\beta = \frac{\vec{\Sigma}.\vec{t}}{||\vec{\Sigma}||} = \frac{P\sin\alpha + F_w\cos\beta_w}{\sqrt{(P\sin\alpha)^2 + 2P\sin\alpha.F_w\cos\beta_w + F_w^2}}. \tag{5}$$

Limit cases of this general formula are easy to check: a situation with no wind ($F_w = 0$) gives $\cos\beta = 1$, which means the drop follows the weight; a situation with a

horizontal window ($\alpha = 0$) gives $\cos\beta = \cos\beta_w$ which means the drop slides in the direction of the wind.

The drop will then move upwards if $90° \leq \beta \leq 180°$ which means $\cos\beta \leq 0$. Therefore, the condition for an upward trajectory given by equation (6) is expressed as follows:

$$P\sin\alpha + F_w\cos\beta_w \leq 0. \quad (6)$$

Since α is taken between 0° and 90°, this condition yields $\cos\beta_w \leq 0$, which corresponds to the intuitive condition that the wind must have a vertical component directed upwards.

2.8 Direction of the drop once dislodged: experimental setup

The acrylic board was placed vertically in front of the wind blower, the inclination was therefore $\alpha = 90°$. The direction of the wind was kept horizontal throughout the experiment ($\beta_w = 90°$). We put a drop of known volume Ω, small enough so that it held on the vertical plane: a first round of trials was performed with 25 μL drops, and another one with 20 μL drops. Colored water was used to increase the contrast. We suddenly let the wind blow at a given speed u, strong enough to dislodge the drop (from 12 to 30 m s^{-1}). Taking a video in front of the plane, we had access to the trajectory of the drop, more precisely to the angle β the trajectory of the drop made with the vertical. One time-lapse photography obtained from the video can be seen in Figure 5.

Equation (5) becomes in the particular case of this setup $\cos\beta = \frac{P}{\sqrt{P^2+F_w^2}} = \frac{P}{||\vec{\Sigma}||}$ or in its equivalent form:

$$\tan\beta = \frac{F_w}{P}. \quad (7)$$

2.9 Global condition

Finally, two conditions need to be fulfilled to observe a drop going up on a car window:
– the drop is dislodged when: $||P\sin\alpha\vec{t} + \vec{F}_w|| \geq F_{ad}$
– the drop goes up when: $P\sin\alpha + F_w\cos\beta_w \leq 0$

3 Results

3.1 Adhesion force

The experimental data for the angle α_s needed to dislodge a given drop are shown on Figure 6.

We noticed a high variability of results. Some drops seem to stay stuck on some irregularities on the surface, which enables them to stay on a higher inclination. This effect will be discussed later on.

We observed two main regimes: for a drop of volume greater than about $17 \pm 1\mu$L, the drop slides when the angle $\alpha_s \leq 90°$ is reached. On the contrary, a smaller drop holds even when the plane reaches the vertical position. Such a drop does not slide at all under its own weight, we thus cannot define an angle of sliding α_s; therefore, this situation is not represented on the graph. However, we draw a vertical line to enhance the change in regime at the limit size.

For drops big enough to slide, we indeed see a clear dependency of the inclination α_s on the volume Ω of the drops, as predicted in equation (2): bigger drops begin to slide at smaller inclination angles.

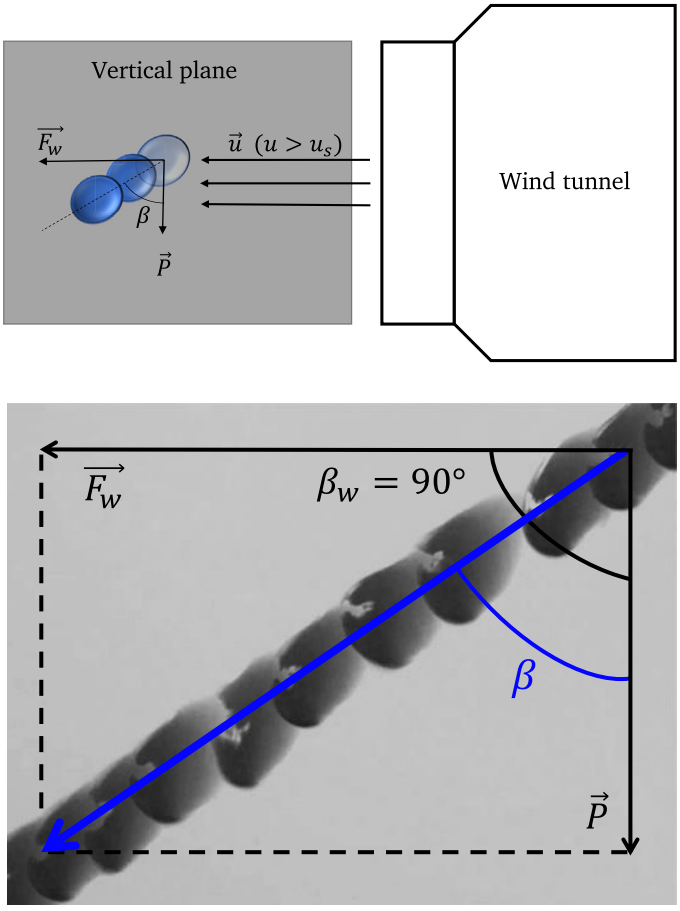

Fig. 5. (Top) schematic view of the experiment performed in order to measure the direction taken by a drop when dislodged by an horizontal wind. The support is maintained vertical. (Bottom) time-lapse photography of a drop in motion on a vertical plane under an horizontal wind. β_w is the angle the wind makes with the vertical, while β is the angle which the sliding drop takes.

3.2 Drag force on the drop

Studying the minimum air speed needed to dislodge a given drop of volume Ω, we observe that bigger drops tend to be dislodged under weaker wind speeds, see Figure 6. For each volume data point, we tested three drops. As for the experiment on adhesion forces, one may notice the large uncertainties on the graph, which stem from the distribution of adhesive forces created by surface imperfections.

3.3 On a vertical plane – both weight and wind

Figure 6 shows the experimental data for the direction β taken by a drop of volume Ω put on a vertical plane in front

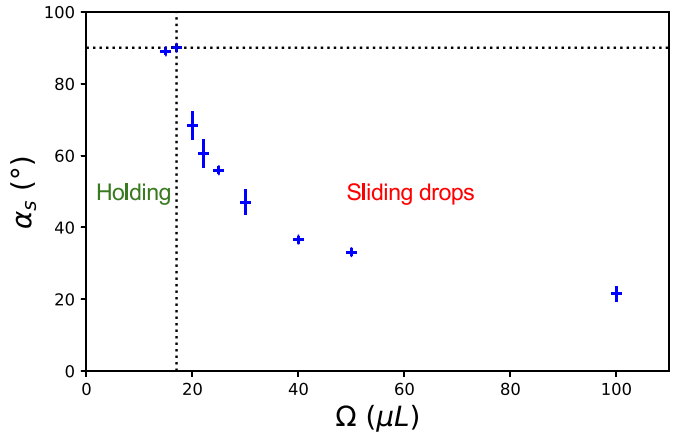

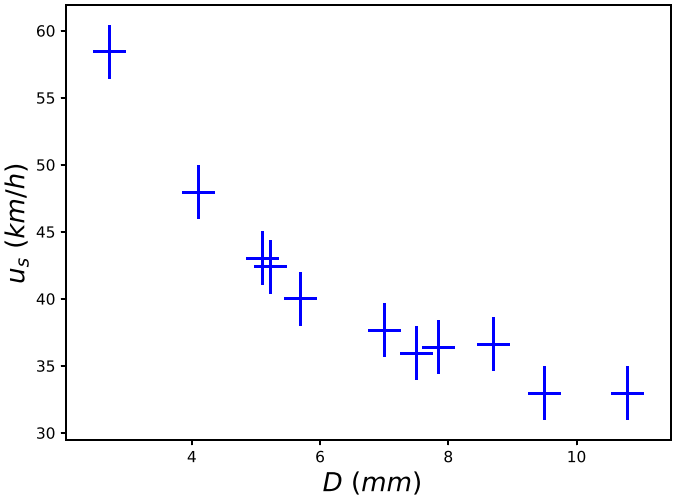

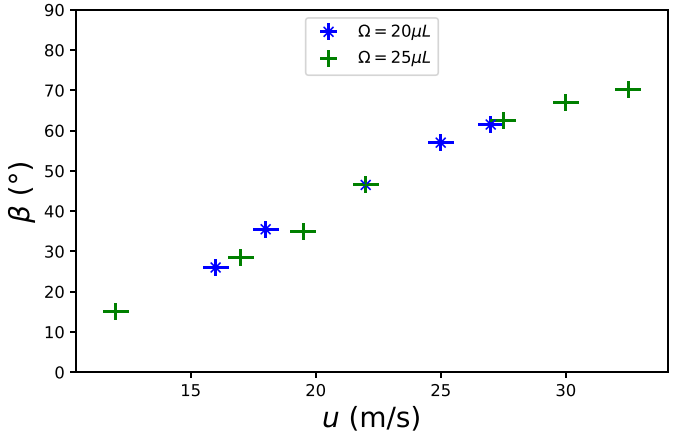

Fig. 6. (Top) a plot of α_s, the inclination needed to dislodge a drop of water, is plotted against the volume Ω of the drop, put on a plane of acrylic. Dashed lines indicate limits for definition of α_s, which cannot exceed 90° (in this case the drop will not fall under its weight). Thus for volumes on the left of the vertical dashed line, α_s is not defined. (Middle) a plot of us, the minimum wind speed needed to dislodge a drop, is plotted against the diameter D of the drop lying on a plane of acrylic. (Bottom) the direction, taken by a drop of volume put on a vertical plane in front of a blower, is plotted against the speed u of the wind. Two values of the volume are used (blue dots: 20μL, and green crosses: 25μL).

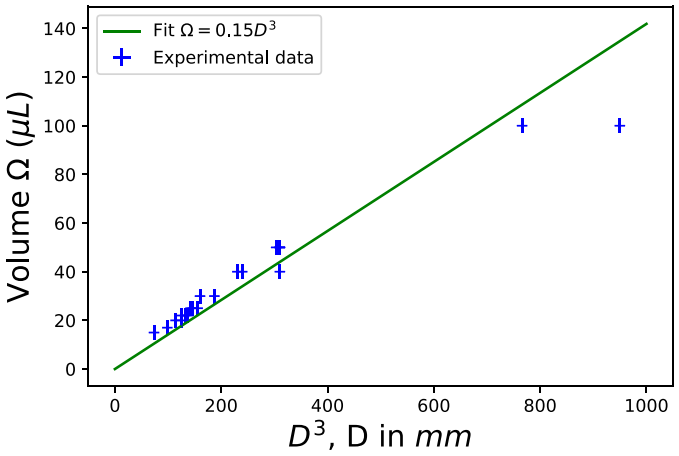

Fig. 7. Experimental law between the volume Ω and the diameter D of a drop defined as the diameter seen from above the drop as it is lying on a horizontal floor. $\Omega \propto D^3$ is a consistent model for small enough drops. Fit does not take into account the two last points, where drops are so big that they spread under their own weight.

of the blower, plotted against the wind speed u. As foreseen in *Methods* with equation (7), the stronger the wind blows, the more the drop tends to follow the direction of the wind (that is β comes closer to 90°).

4 Discussion

4.1 Scaling laws

In the following paragraphs, we want to simplify the equations of the first section into scaling laws, hoping it will help understand the dependence of minimum wind speed u_s, maximum inclination α_s and direction of motion β regarding the different parameters. We therefore need a relation between the volume Ω, the projected surface S and the diameter D of a drop lying on a plane.

We assess in first approximation that the drops are small enough to be considered as half-spheres of diameter D. Thus, the volume is expected proportional to D^3 and the projected surface as D^2. We poured drops of known volume and measured the diameter by taking pictures from above. Figure 7 shows the relation we obtained between the diameter and the volume of the drop.

The experimental data are in good agreement with the approximation $\Omega = aD^3$ (with a is a dimensionless geometrical constant), as long as the drop is not too big. When the drop is about five times the capillary length $L_c \approx 2.7$ mm, the drop spreading under its own weight is not negligible. Its width becomes much smaller than its radius, the model of the half sphere is no longer valid. This explains why the points of $\Omega = 100\,\mu$L are far from the fit $\Omega = aD^3$. Our simple approximation of half-spherical drops is thus accurate for volumes smaller than 50 μL, that we used in our experiments. In the following models, we now assess that:

$$\Omega \propto D^3 \tag{8}$$

4.2 Interpretation of results in scaling laws

4.2.1 Adhesion force

We can rewrite the equation (2) obtained in Section 2 in a more convenient way:

$$\sin\alpha_s = \frac{\gamma}{\rho g}(\cos\theta_r - \cos\theta_a)\frac{D}{\Omega}$$

The factor $\cos\theta_r - \cos\theta_a$ is only due to the interaction between water and the material of the plane used for the experiment. It is considered as a fixed constant during our experiment, since we used the same plane each time. By using the relation (8) between the volume and the diameter, and denoting $L_c = \sqrt{\gamma/\rho g}$ the capillary length, we obtain the following scaling law:

$$\sin\alpha_s \sim L_c^2\frac{D}{\Omega} \sim L_c^2\Omega^{-2/3} \tag{9}$$

Plotting $\sin\alpha_s$ depending on $\Omega^{-\frac{2}{3}}$, as done in Figure 8 shows a linear relationship as expected. This scaling law (9) indicates that the expression of the adhesion force as a force proportional to the diameter of the drop is relevant.

4.2.2 Drag force

Once again, we can simplify the theoretical equation (3) obtained in Section 2 into a scaling law. As an expression for the speed of the wind u_s needed to dislodge a drop of volume Ω on an horizontal plane, we obtain:

$$u_s^2 \sim \frac{D}{S} \propto \Omega^{-1/3}. \tag{10}$$

We can now plot our data again according to equation (10) and check that we have a linear relation between u_s^2 and $\Omega^{-1/3}$. Figure 8 shows that our data are consistent with a linear law. Consequently, our expression for the drag force proportional to the projected surface of the drop is validated.

4.2.3 Direction β under an horizontal wind

In order to check the relations obtained on $\tan\beta$ on a vertical plane with a strong horizontal wind, equation (7) can be simplified. Using the above determined expressions for drag force and weight in scaling laws, it gives:

$$\tan\beta = \frac{F_w}{P} = \frac{C_x\rho_a}{2\rho_{\text{water}}g}\frac{Su^2}{\Omega} = \frac{1}{g^*}\frac{u^2}{\Omega^{1/3}} \tag{11}$$

where $g^* = \frac{2\rho_{\text{water}}}{C_x\rho_a}g$ is a reduced acceleration. Drag coefficients for drops are given in [1] and estimated to 0.1–0.2 for a drop of water on a plane surface. For a drag coefficient of $C_x = 0.15$ we have $g^* \approx 1.3\times10^5$ m s^{-2}. We thus plot $\tan\beta$ according to the ratio $u^2\Omega^{-1/3}/g^*$ in Figure 8.

The relation is indeed linear, as predicted by the scaling law (11). This scaling law is one more argument in favor of the global relationship (5) which gives the direction of the drop depending on its volume and the speed of the wind.

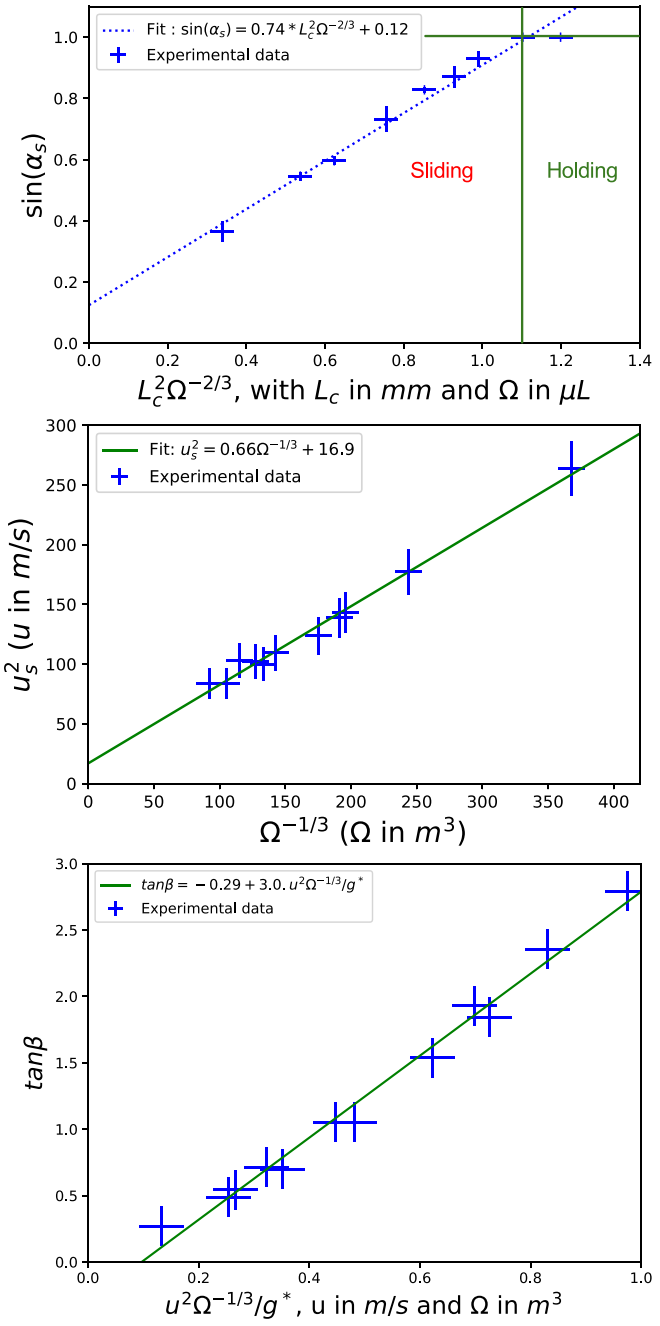

Fig. 8. (Top) scaling of $\sin\alpha_s$ (α_s the sliding angle for a drop) as a function of $L_c^2\Omega^{-\frac{2}{3}}$, with L_c the capillary length for water under normal conditions of pressure and temperature. Values of Ω range from 15 μL to 100 μL. A linear fit (dashed line) to experimental data is expected, according to our theory. (Middle) experimental law for the relation between wind speed u_s and drop volume Ω on an horizontal plane, law stemming from the competition between the drag force and the adhesion force. Linear correlation (red line) is consistent with our theoretical model. (Bottom) experimental results on the angle β taken by drops of given volume Ω under an horizontal wind u. Drops small enough are set on a vertical plane (we took $\Omega = 20$ μl or 25 μl so they can stay DESPITE GRAVITY). Then the wind blower is switched on, and blows horizontally with a speed u bigger than $u_s(\Omega)$, the minimum value needed to dislodge the drop. As our model predicts, there is a linear law between $\tan\beta$ and the ratio $u^2\Omega^{-1/3}/g^*$.

4.2.4 On the complete model

The individual motion of a drop deposited on a plane seems to be rather well described by the above presented theory: wind and gravity compete with the adhesion force to put the drop in movement. The initial direction of the drop is then given by a global relation (11) between the angle of motion β and the ratio $u^2/(\Omega^{1/3}g^*)$.

For a given value of a horizontal wind speed, say $u = 50\,\text{km/h}$, drops under 3 mm diameter will not detach, drops between 3 mm and 4.5 mm diameter will have an initial direction closer to the wind ($\beta > 45\,°$), while drops over 4.5 mm diameter will be more sensitive to gravity ($\beta < 45\,°$). For $u = 100\,\text{km/h}$, the limit for being more sensitive to the wind is $D < 17\,\text{mm}$, which is the case of most drops on a car window.

For a drop of fixed volume (say $20\,\mu$l), the trajectory will mostly follow the wind ($\beta > 45\,°$) only if $u > 42\,\text{km/h}$. These figures are obtained after the fit given in Figure 8, with numerical values on an acrylic board.

From there, we can deduce properties of the actual motion of rain drops on the side window of a car. Two major trends may be mentioned:

– *Dependence on the drop volume*: the general trend resulting from equations (9) and (10) is that smaller drops tend to be more attached to the window than bigger ones. Bigger drops are easier to dislodge than smaller one, and their trajectory is more susceptible to the influence of weight. Indeed the weight scales in D^3, so it grows quicker than the drag force which scales in D^2 and than the adhesion force (proportional to D). The volume of the drop thus has a critical role in the problem in so far as it determines both the transition between the static and dynamical behaviors and the direction taken by the drop when put in motion.
– *Dependence on the car speed*: we conducted experiments to assess the importance of the speed u of the wind actually pushing the drop. This parameter is critical, on an equal footage with the volume, as it influences both the detaching and the direction taken by the drop. The speed u grows with the speed of the car on a real situation, yet a more precise correlation would require advanced numerical simulation of the vortices against the car window, which is far from our reach.

4.3 Dead ends

One may wish to extend the model to the complete description of a population of drops on a car window. Such a description should satisfyingly address the following points, which our model cannot exactly account for.

4.3.1 Influence of surface nature and treatment

When writing equation (2), we regard the factor $\cos\theta_r - \cos\theta_a$ as a dimensionless constant, depending only on the chemical interactions between the surface and the drop, which does not play any role in the following scaling laws [Eqs. (9) and (3)]. Yet of course this factor's scale has a prominent role to play in the motion of the drop. Indeed, equation (2) states the existence of a minimal volume for water drops to detach under gravity, depending on surface nature and treatment.

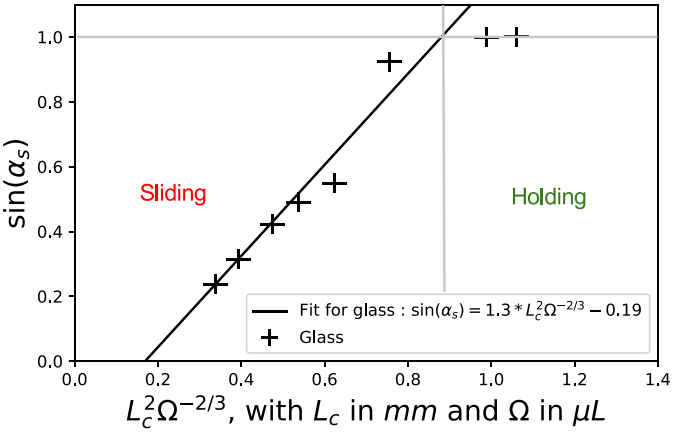

Fig. 9. Experimental results for the inclination α_s needed to dislodge a drop of volume Ω, put on an initially horizontal plane of glass that we slowly inclined. Ω ranges from 15 μL to 100 μL. This graph shows that for a glass surface, the scaling law between $\sin\alpha_s$ and $L_c\Omega^{-2/3}$ is once again reasonably valid (as it was for a plane of acrylic). What changes, compared to the previous experimental results with a plane of acrylic, is the slope of the fit. This slope is indeed linked to the contact angles between water and the plane, which are different for a plane of glass and acrylic.

We conducted experiments and verified our model with acrylic. It is noteworthy that the same law holds for other surfaces. We checked it out experimentally with normal glass, as can be seen in Figure 9. This enables us to extend the expression of adhesion force to any kind of ideal surface, from regular glass to car glass, or to glass treated to be hydrophobic, as may be the case for a luxury car. Only the coefficients of proportionality may change from one surface to another, as long as imperfections are neglected.

Complex models of the contact angles have been developed, namely by de Gennes [14] and Cox [15], which quantitatively relate the contact angles to the properties of the fluid and the size of the contact line of the drop with the surface. However, these variations have no impact on the physics we presented.

The wear of the surface may also play a significant role on the behavior of the drops. As mentioned in Section 3, we noted that imperfections such as millimeter sized scratches on the surface may force the drops to stick under bigger external constraints (weight or drag). Indeed the geometry of the contact zone between the drop and the plane is modified by the presence of the scar, and the surface of contact is usually enhanced. Since there is no perfectly smooth surface, the size of imperfections contact line with the drop is a crucial parameter for pinning and depinning mechanisms, as has been studied by Paxton and Varanasi in [16].

4.3.2 Drops size distribution and merging

We have focused our study on the motion of an individual drop on a car window. For a better understanding of the

global phenomena showed in Figure 1, it would be necessary to take into account the influence of the other drops. The presence of a drop on the path of a first drop of comparable size will impact its direction: the two drops will touch and merge. As the resulting drop has grown in size, the weight takes more importance compared to wind drag (it scales in D^3, so grows quicker than the drag force which scales in D^2): the drop's direction tends to turn downwards. Furthermore, the trajectory of drops go suddenly up and down (even if only on a few mm) while they merge with surrounding drops, which creates erratic-looking behaviors. A model for the dynamics of merging drops can be found in [1].

It would be interesting to have access to a size distribution of drops on a window. Though models for the size of drops in a rainfall exist since long (see for example [17]), this is unfortunately no easy task. We can however give some simple idea: the quicker the car moves, the stronger the local wind, and the smaller the drops which stay stuck on the window. Furthermore, drops tend to splash out more violently when they impact the car at higher speeds, which may also increase the proportion of small drops on the window for high car velocities.

Besides, some parts of the window are wet, covered by a thin layer of water or by a rivulet. It is energetically interesting for the drop to go on such a wet surface, as the interfaces between glass/water and water/air are already existing. As mentioned in the introduction, we have not tackled these aspects in this paper.

4.3.3 Air flow around the car

Cars have very different shapes, and this has a great influence on the air flow, and therefore on the local wind on the size window. This is why the global behavior of drops on one car may be different from drops on another car, and totally differs from drops on trucks.

The influence of the car geometry has been studied by Gilliéron and Kourta [8]. He has shown that on conventional cars, a vortex forms at the junction between the windscreen and the side window. Whatever the car model considered, this vortex always has the same direction of rotation, which yields an upside component of the wind speed on the side window. This is the reason why some of the drops can be seen going up against gravity: there are indeed regions of the window with strong upwards wind.

As the photo of an experiment illustrates in Figure 10, the wind direction is not uniform on a window. Its value depends on the position of the drop of the window as well, and on the car model considered.

The main difficulty encountered in developing our theory further was to accurately estimate the wind along the car window. We first tried to measure the dependence between the magnitude of the upward wind speed and the magnitude of the car speed using an anemometer. We obtained the expected coarse correlation between the two: the wind speed increases when the car moves faster. However, the dimensions of the anemometer (a few decimeters) are not the least negligible given the Reynolds number of the flow. Therefore, the presence of the device itself modifies the geometry of the flow. This prevents us from getting accurate measures on the upward flow against the car, all the more so as we were forced to open the window on a small length to hold the anemometer. We then tried to simulate Navier–Stokes equations with a Computing Fluid Dynamic software, but we were not able to obtain enough precision so as to predict the formation of vortices studied in the literature [8].

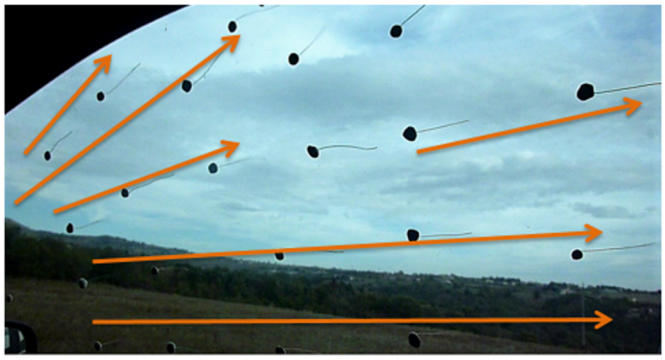

Fig. 10. Photography from an experiment we conducted in a real car, driving at 90 km/h on a straight road. Little cotton threads had been previously stuck on the outside surface of the window. They show the direction of the local wind. On the picture, orange arrows are added for a better visualization of the direction of the threads.

One more step which could account for the erratic trajectories of a population of drops would be to take the drop-induced flow modification (as studied experimentally in [18]) into account while doing simulations. However, this is once again far from our reach.

5 Conclusion

The present work gives the basis for further study of the motion of a population of drops on the side window of a car. We developed a simple model taking into account the weight, drag force and contact force undergone by a single drop sticking on a plane. Applying the equations of motion yielded consistent experimental results regarding the initial direction taken by the drop. We explicitly showed the dependence of the motion on the main parameters of the problem: the volume and diameter of the drop – that we treated as a single parameter in first approximation – and the speed of the wind against the window.

We showed that three distinct regimes exist for fixed condition of wind speed. On an acrylic board for instance, if $u = 50\,\mathrm{km/h}$, small drops ($D < 3\,\mathrm{mm}$) will stick to the surface and would not move, medium size drops ($3 < D < 4.5$ mm) will mostly follow the wind and large drops ($D > 4.5$ mm) will be more sensitive to gravity than wind.

We also showed there is a variability of the detaching parameters due to the surface state of the window.

Being given a map of the wind on the window, the size and initial position of a single drop, our model should be able to predict its trajectory, assuming quasistatic motion,

through point-to-point approximation. The complete problem of raindrop motion will be the object of future research: taking into account the size distribution of drops on the window, the local inclination of the plane on which each drop stands and the complete velocity field of the wind against the car will enable further studies to explore the movement of a whole population of drops on the side window. This would allow to optimize both surface treatment and window geometry to evacuate drops faster.

This work is based on one of the problems proposed in the 2018 edition of the International Physicist' Tournament (IPT), a scientific competition open to students. The problem in question was stated as follows : "*When a car moves with high speed in rain sometimes the drops on its side window walk up but not down. Explain the phenomenon and find the conditions for it to occur (size of the drops and the car speed for example). What determines the drop trajectory and how does it depend on the important parameters?*". Following the guidelines imposed by the IPT, we investigated the motion of rain drops on a car side window from the point of view of this final question, and focused on the direction taken by the drops once they undergo a strong wind coupled to gravity.
We are grateful to Pierre Lecointre, Christophe Clanet, from the LadHyX, Guilhem Gallot from the LOB, and Fabian Cadiz from the PMC at Ecole polytechnique, for the help they provided during the project and then for the fruitful commentaries and corrections they brought to the core of this article. We also thank Pierre Gilliéron, from Renault, as well as Barbara Brudieu and Alban Sauret, from Saint-Gobain, for their helping us on understanding better automobile aerodynamics and glass wetting.

References

1. A.K. Njifenju, Gouttes et films liquides en aérodynamique automobile, PhD thesis, ESPCI, 2010
2. S.C. Yih, Phys. Fluids **6**, 321–334 (1963)
3. N. Le Grand-Piteira, A. Daerr, L. Limat, Phys. Rev. Lett. **96**, 254503 (2006)
4. T. Podgorski, Ruissellement en conditions de mouillage partiel, PhD thesis, Université Pierre et Marie Curie – Paris VI, 2000
5. C.G.L. Furmidge, J. Colloid Sci. **17**, 309–322 (1962)
6. P.A. Durbin, J. Fluid Mech. 196–205 (1988)
7. J. Fan, M.C.T. Wilson, N. Kapur, J. Colloid Interface Sci. **356**, 286–292 (2011)
8. P. Gilliéron, A. Kourta, Aérodynamique Automobile pour l'environnement, le Design et la sécurité Cépadués (2014)
9. A. Gauthier, Hydrophobie dynamique et dynamiques hydrophobes, PhD thesis, Ecole polytechnique, 2015
10. S. Chandra, C.T. Avedisian, Proc. R. Soc. Lond. 432, 13–41 (1991)
11. G. MacDougall, C. Ockrent, Proc. R. Soc. Lond. **180A**, 151 (1942)
12. L. Prandtl, NACA TM 452, 1928
13. S.F. Hoerner, Fluid-dynamic drag, Hoerner Fluid Dynamics, New York, 1965
14. P.G. De Gennes, C. R. Acad. Sci. **288(IIb)**, 219 (1979)
15. R.G. Cox, J. Fluid Mech. **168**, 169–220 (1986)
16. A.T. Paxton, K.K. Varanasi, Nat. Commun. **4**, 1492 (2013)
17. J.S. Marshall, W. McK. Palmer, Nat. Commun. **5**, 1492 (1948)
18. H. Alireza, L. Sungyon, Phys. Rev. Fluids **2**, 196–205 (2017)

Cite this article as: Julie André, Clément Brochet, Quentin Louis, Amaury Barral, Anthony Guillen, Fang-Ting Goh, Angel Prieto, Thibault Guillet, Motion of rain drops on a car side window, Emergent Scientist **3**, 3 (2019)